Endofullerenes

DOI: 10.1002/anie.200906325

Spin Divergence Induced by Exohedral Modification: ESR Study of $Sc_3C_2@C_{80}$ Fulleropyrrolidine**

Taishan Wang, Jingyi Wu, Wei Xu, Junfeng Xiang, Xin Lu, Bao Li, Li Jiang, Chunying Shu, and Chunru Wang**

Endohedral metallofullerenes have attracted wide interest because of their novel structures and potential applications in a variety of fields, such as nanotechnology and biomedical applications.[1–3] Exohedral functionalization plays a critical role not only in improving solubility and processability of metallofullerenes for expanding their practical applications, including photovoltaic cells,[4] magnetic resonance imaging agents,[5] and radiotracers,[6] but also in controlling the position of encapsulated atoms and corresponding properties. Thus, the characteristics of endofullerenes become more diversified, and these help in designing novel materials with controllable electronic and magnetic properties.[7–13] The abundant dimetal-encapsulated and trimetallic nitride template encapsulated C_{80} species and their derivatives have been studied in detail.[1–3,7–10] However, little was known about the derivatives and corresponding properties for the metal carbide encapsulated fullerenes, such as $Sc_3C_2@C_{80}$, even though its pristine structure has been studied in detail since its discovery.[14–20] In view of its elusive structure and alluring ESR spectrum, it is significant to investigate the effect of exohedrally functional groups on the elusive structures and properties of $Sc_3C_2@C_{80}$.[17–20]

Herein, we report the spin divergence in $Sc_3C_2@C_{80}$ fulleropyrrolidine induced by exohedral modification by the Prato reaction.[21,22] The structure of $Sc_3C_2@C_{80}$ fulleropyrrolidine was characterized by NMR, UV/Vis, and IR spectroscopy, as well as theoretical studies.

The synthesis of $Sc_3C_2@C_{80}$ fulleropyrrolidine was carried out in *o*-dichlorobenzene with a solution of $Sc_3C_2@C_{80}$, *N*-ethylglycine, and ^{13}C-enriched paraformaldehyde. The product was isolated and purified by high performance liquid chromatography (HPLC) and identified as fulleropyrrolidine monoadduct by matrix-assisted laser desorption ionization time-of-flight (MALDI-TOF) mass spectrometry (Figure 1).

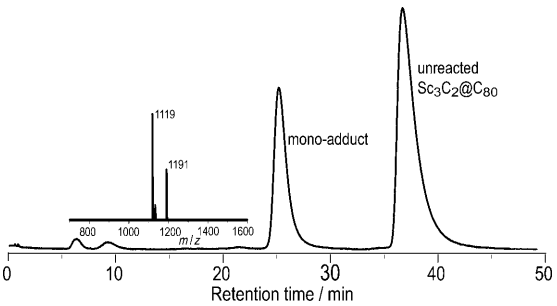

Figure 1. HPLC profile of reaction mixture (*N*-ethylglycine and ^{13}C-enriched paraformaldehyde) treated with $Sc_3C_2@C_{80}$ for 10 min. The insert shows the MALDI-TOF mass spectrum for the monoadduct.

Although the $Sc_3C_2@C_{80}$ fulleropyrrolidine monoadduct is paramagnetic, the ^{13}C NMR spectrum exhibits a singlet at $\delta =$ 71.62 ppm for the ^{13}C-labeled methylene carbon (Figure 2),

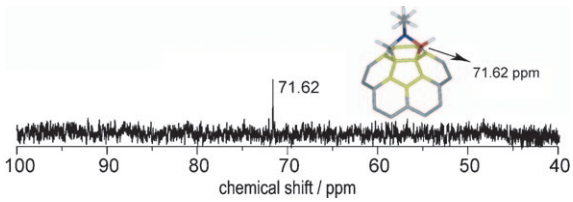

Figure 2. ^{13}C NMR spectrum of ^{13}C-labeled $Sc_3C_2@C_{80}$ fulleropyrrolidine monoadduct. The insert depicts the partial structure of the monoadduct. The yellow bonds show the adjacent 5- and 6-membered rings around the addend, and the red atom represents the ^{13}C-labeled methylene carbon atom.

indicating that the low spin density distribution of cluster close to the addend does not significantly affect the pyrrolidine group, and the 5,6-ring junction is the reaction site for $Sc_3C_2@C_{80}$ fulleropyrrolidine as in pyrrodino $Sc_3N@C_{80}$-I_h case.[23,24] The heteronuclear multiple quantum coherence (HMQC) spectrum verifies the non-equivalent methylene protons attached to the equivalent methylene carbon atoms, which is consistent with the 5,6-ring addition assignment of the fulleropyrrolidine (see the Supporting Information).

Noticeably, although the geminal methylene protons on the pyrrolidine ring of the $Sc_3C_2@C_{80}$ fulleropyrrolidine

[*] Dr. T.-S. Wang, Dr. J.-Y. Wu, Dr. W. Xu, Dr. J.-F. Xiang, Dr. B. Li, Dr. L. Jiang, Prof. Dr. C.-Y. Shu, Prof. Dr. C.-R. Wang
Institute of Chemistry, The Chinese Academy of Sciences
Beijing, 100190 (China)
Fax: (+86) 10-6265-2120
E-mail: shucy@iccas.ac.cn
crwang@iccas.ac.cn
Homepage: http://spm.iccas.ac.cn/english/members/crwang.htm
Prof. Dr. X. Lu
State Key Laboratory of Physical Chemistry of Solid Surface
Center for Theoretical Chemistry, Department of Chemistry
Xiamen University, Xiamen, 361005 (China)

[**] We thank Dr. Lai Feng and Dr. Ning Chen for valuable discussions. This work was supported by the 973 Program (2006CB300402), NSFC (20821003, 20702053), Important National Science & Technology Specific Projects (2008ZX05013-004), and the Chinese Academy of Sciences.

Supporting information for this article is available on the WWW under http://dx.doi.org/10.1002/anie.200906325.

WILEY InterScience DISCOVER SOMETHING GREAT
© 2010 Wiley-VCH Verlag GmbH & Co. KGaA, Weinheim

monoadduct exhibit similar chemical shifts and splitting pattern to that of $Sc_3N@C_{80}$-I_h analogue,[23,24] the chemical shift difference ($\Delta\delta = 4.39–3.04 = 1.35$) of the methylene geminal protons is larger than that of $Sc_3N@C_{80}$-I_h fulleropyrrolidine ($\Delta\delta = 4.07–2.81 = 1.26$). Besides the different ring currents derived from the adjacent 5- and 6-membered rings,[24,25] the different encapsulated metal clusters also should contribute to this large degree of deshielding/shielding effect.

Fourier transform infrared (FTIR) spectroscopy was employed to elucidate the structures of $Sc_3C_2@C_{80}$ and $Sc_3C_2@C_{80}$ fulleropyrrolidine (see the Supporting Information). For $Sc_3C_2@C_{80}$ fulleropyrrolidine monoadduct, signals at around 693 and 714 cm^{-1} represent the antisymmetric Sc–C stretching vibrations, which are different from that of pristine $Sc_3C_2@C_{80}$ with single signal at 670 cm^{-1}. This change can be ascribed to the changed configuration of Sc_3C_2 cluster resulting from the exohedral addend.

The geometry of the $Sc_3C_2@C_{80}$ fulleropyrrolidine monoadduct was further investigated by DFT calculations.[26,27] The results demonstrate that the molecule has a mirror plane splitting the pyrrolidine ring, and the Sc_3C_2 endocluster has C_{2v} symmetry, reduced from C_{3v} symmetry in pristine $Sc_3C_2@C_{80}$ (Figure 3).[17–20] For the inner Sc_3C_2 cluster, one

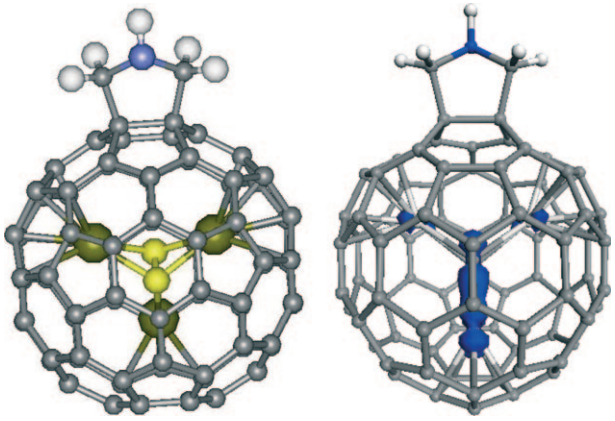

Figure 3. Optimized structure (left; N blue, Sc yellow, C gray, H white) and calculated spin density distribution (right) of the $Sc_3C_2@C_{80}$ fulleropyrrolidine monoadduct.

Sc atom is located at bottom of the cage and far away from the addend; and the other two Sc atoms are close to the pyrrolidine ring and positioned symmetrically. Such an assignment of inner cluster is consistent with the electrostatic potential map for the calculated 5,6-adduct of $[C_{80}(CH_2)_2NH]^{6-}$,[28] for which the electrostatic potentials have a minimum at the bottom of the cage and far away from the addend, thus leading to one Sc atom located near the energy minimum and the other two Sc atoms repulse from each other to minimize the energy further.[28] Therefore, the chemical functionalization on metallofullerene $Sc_3C_2@C_{80}$ can change the configuration of the inner Sc_3C_2 cluster effectively and can be used to control the location of Sc atoms intentionally.

Figure 4 shows the experimental and simulated ESR spectra of the $Sc_3C_2@C_{80}$ fulleropyrrolidine monoadduct. Surprisingly, the spectra of monoadduct and pristine

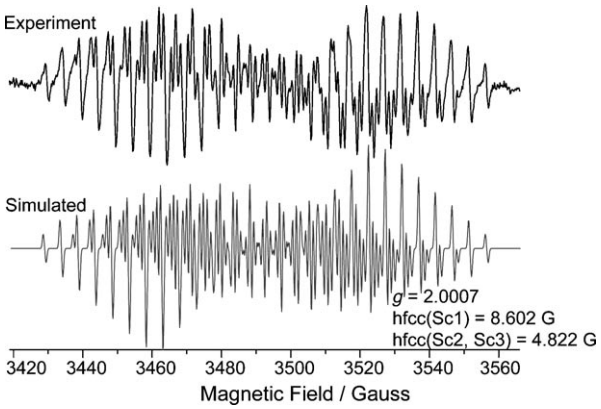

Figure 4. Experimental and simulated ESR spectra of the $Sc_3C_2@C_{80}$ fulleropyrrolidine monoadduct.

$Sc_3C_2@C_{80}$ differ substantially (Table 1).[14–16] Splitting values of 8.602 (one nucleus) and 4.822 G (two nuclei) and a g value of 2.0007 were observed for the $Sc_3C_2@C_{80}$ fulleropyrrolidine

Table 1: Scandium hyperfine coupling constants (α_{Sc}) and g values of pristine $Sc_3C_2@C_{80}$ and $Sc_3C_2@C_{80}$ fulleropyrrolidine.[a]

Sample	α_{Sc} [G]	g value
$Sc_3C_2@C_{80}$	6.256 (6.51[b])	2.0006 (1.9985[b])
monoadduct	8.602; 4.822; 4.822	2.0007

[a] All experiments were performed at room temperature in *o*-DCB. [b] The α_{Sc} and g values of $Sc_3C_2@C_{80}$ are taken from reference [15] and were measured at 220 K in CS_2.

monoadduct, compared with 6.256 G (three nuclei) and 2.0006, respectively, for $Sc_3C_2@C_{80}$. This ESR pattern of $Sc_3C_2@C_{80}$ fulleropyrrolidine is also different from that of $Sc_3C_2@C_{80}$(Ad) (Ad = adamantylidene) (20.55, 5.479 MHz). As the hyperfine coupling constants (hfcc) of Sc nuclei are related to the spin density near the Sc atoms, the spin density distributions were calculated to elucidate the paramagnetic property of $Sc_3C_2@C_{80}$ fulleropyrrolidine. As shown in Figure 3, the spin density for $Sc_3C_2@C_{80}$ fulleropyrrolidine is localized exclusively on the Sc_3C_2 endocluster inhomogeneously; the higher spin density is localized on a unique Sc nucleus far away from the pyrrolidine addend, whereas the lower spin density is localized on the other two Sc nuclei homogeneously. In contrast, the pristine $Sc_3C_2@C_{80}$ has the most spin localization on the Sc_3C_2 cluster as well but each Sc nucleus has the same spin density.[19] Therefore, remarkably, the spin divergence in $Sc_3C_2@C_{80}$ fulleropyrrolidine was induced by exohedral modification, and these unique spin density distributions derived from the exohedral modification can well explain the coupling constants of Sc nuclei in

 © 2010 Wiley-VCH Verlag GmbH & Co. KGaA, Weinheim

$Sc_3C_2@C_{80}$ fulleropyrrolidine monoadduct. Notably, although $Sc_3C_2@C_{80}$ fulleropyrrolidine is paramagnetic, the very low spin density on fullerene cage close to the addend could explain the ^{13}C NMR signal at $\delta = 71.62$ ppm for the ^{13}C-labeled methylene carbon. Again, chemical modification has been proved to be a powerful technique not only to change the configuration of inner cluster, but also to tune the electronic and paramagnetic properties of an endofullerene.

Comparisons of the spin density distributions between paramagnetic trimetallic endofullerenes are helpful to understand the unique ESR properties of $Sc_3C_2@C_{80}$ fulleropyrrolidine. The $Y_3N@C_{80}$-I_h fulleropyrrolidine monoanion was reported to be ESR active with hfcc patterns of 6.26 G (two nuclei) and 1.35 G (one nucleus),[29] and the unpaired spin was delocalized both on the fullerene cage and on the internal Y_3N cluster.[29] The $Sc_3N@C_{80}$ anion radical was reported to be ESR active with peculiar hfcc pattern of 55.7 G (three nuclei), and the exclusive unpaired spin was proposed to be on the Sc_3N cluster.[30,31] In contrast, the $Sc_3N@C_{68}$ cation radical was reported with hfcc of 1.289 G (three nuclei), and its unpaired spin was delocalized both on the C_{68} cage and on the endocluster as in the $Y_3N@C_{80}$-I_h fulleropyrrolidine monoanion case.[32] From the above examples, we can conclude that the unpaired spin distributions are relevant to the kind of endoclusters and type of fullerene cages.

For $Sc_3C_2@C_{80}$, the Sc_3C_2 cluster can rotate freely as confirmed by ESR, MEM/Rietveld, and ^{13}C NMR spectroscopic experiments, as well as DFT calculations. This dynamic Sc_3C_2 cluster along with the equivalent coupling between the three Sc atoms and the unpaired electron leads to symmetrical hyperfine splitting of 22 lines.[14–20] In contrast, the splitting pattern for $Sc_3C_2@C_{80}$ fulleropyrrolidine suggests that the exohedral addend prominently hinders the free rotation of the endocluster, which leads to inhomogeneous spin density distributions on internal cluster. The peculiar chemical shift difference between the methylene geminal protons also suggests a nonhomogeneous C_{80} cage caused by hindered Sc_3C_2 rotation. Unlike the proposed jumping motion for the three Sc atoms in pristine $Sc_3C_2@C_{80}$, intrafullerene motion of Sc atoms in $Sc_3C_2@C_{80}$ fulleropyrrolidine was suggested as oscillation modes by DFT calculation (see the Supporting Information). The Sc_3C_2 cluster oscillates randomly around the equilibrium position; for example, the C_s plane of Sc_3C_2 cluster can swing to and fro, left and right, as well as around within 15° for the dihedral angles. Therefore, there is no doubt that the unpaired spin is also closely connected to the intrafullerene motion of the endocluster.

In summary, the paramagnetic properties of $Sc_3C_2@C_{80}$ were tuned by exohedral modification. The 5,6-ring junction was determined to be the reaction site for the $Sc_3C_2@C_{80}$ fulleropyrrolidine monoadduct, and the endohedral Sc_3C_2 cluster was deformed by the pyrrolidine addend. Most importantly, the pyrrolidine addend changes the spin density distributions and alters the paramagnetic properties of $Sc_3C_2@C_{80}$ fulleropyrrolidine as a result. The dynamics of Sc_3C_2 endocluster were also discussed to elucidate the variable properties caused by the exohedral addend. Such controllable molecular paramagnetism is of great significance to the construction of novel molecular devices.

Experimental Section

The synthesis of $Sc_3C_2@C_{80}$ fulleropyrrolidine was carried out in a solution of $Sc_3C_2@C_{80}$ (5 mg) in *o*-dichlorobenzene (*o*-DCB) with an excess of *N*-ethylglycine (8 mg) and ^{13}C-enriched (99%) paraformaldehyde (8 mg) at 108°C for 10 min. The product was isolated and purified by HPLC. The ^{13}C NMR and HMQC spectra were measured in CS_2 with D_2O inside a capillary as an internal lock. All the ESR experiments were performed at room temperature in *o*-DCB.

DFT calculations were investigated by Perdew, Burke, and Enzerhof (PBE)/double numerical plus polarization using the DMol^3 code in Accelrys Materials Studio.[26,27]

Received: November 10, 2009
Published online: February 5, 2010

Keywords: carbides · endohedral fullerenes · EPR spectroscopy · exohedral addends · Prato reaction

[1] H. Shinohara, *Rep. Prog. Phys.* **2000**, *63*, 843–892.
[2] N. Martin, *Chem. Commun.* **2006**, 2093–2104.
[3] L. Dunsch, S. F. Yang, *Small* **2007**, *3*, 1298–1320.
[4] R. B. Ross, C. M. Cardona, D. M. Guldi, S. G. Sankaranarayanan, M. O. Reese, N. Kopidakis, J. Peet, B. Walker, G. C. Bazan, E. Van Keuren, B. C. Holloway, M. Drees, *Nat. Mater.* **2009**, *8*, 208–212.
[5] M. Mikawa, H. Kato, M. Okumura, M. Narazaki, Y. Kanazawa, N. Miwa, H. Shinohara, *Bioconjugate Chem.* **2001**, *12*, 510–514.
[6] D. W. Cagle, S. J. Kennel, S. Mirzadeh, J. M. Alford, L. J. Wilson, *Proc. Natl. Acad. Sci. USA* **1999**, *96*, 5182–5187.
[7] M. Yamada, T. Nakahodo, T. Wakahara, T. Tsuchiya, Y. Maeda, T. Akasaka, M. Kako, K. Yoza, E. Horn, N. Mizorogi, K. Kobayashi, S. Nagase, *J. Am. Chem. Soc.* **2005**, *127*, 14570–14571.
[8] T. Akasaka, T. Kono, Y. Matsunaga, T. Wakahara, T. Nakahodo, M. O. Ishitsuka, Y. Maeda, T. Tsuchiya, T. Kato, M. T. H. Liu, N. Mizorogi, Z. Slanina, S. Nagase, *J. Phys. Chem. A* **2008**, *112*, 1294–1297.
[9] M. Yamada, C. Someya, T. Wakahara, T. Tsuchiya, Y. Maeda, T. Akasaka, K. Yoza, E. Horn, M. T. H. Liu, N. Mizorogi, S. Nagase, *J. Am. Chem. Soc.* **2008**, *130*, 1171–1176.
[10] M. Yamada, T. Wakahara, T. Tsuchiya, Y. Maeda, M. Kako, T. Akasaka, K. Yoza, E. Horn, N. Mizorogi, S. Nagase, *Chem. Commun.* **2008**, 558–560.
[11] X. F. Li, L. Z. Fan, D. F. Liu, H. H. Y. Sung, I. D. Williams, S. Yang, K. Tan, X. Lu, *J. Am. Chem. Soc.* **2007**, *129*, 10636–10637.
[12] X. Lu, J. X. Xu, X. R. He, Z. J. Shi, Z. N. Gu, *Chem. Mater.* **2004**, *16*, 953–955.
[13] B. P. Cao, T. Wakahara, Y. Maeda, A. H. Han, T. Akasaka, T. Kato, K. Kobayashi, S. Nagase, *Chem. Eur. J.* **2004**, *10*, 716–720.
[14] H. Shinohara, H. Sato, M. Ohkohchi, Y. Ando, T. Kodama, T. Shida, T. Kato, Y. Saito, *Nature* **1992**, *357*, 52–54.
[15] H. Shinohara, M. Inakuma, N. Hayashi, H. Sato, Y. Saito, T. Kato, S. Bandow, *J. Phys. Chem.* **1994**, *98*, 8597–8599.
[16] T. Kato, S. Bandou, M. Inakuma, H. Shinohara, *J. Phys. Chem.* **1995**, *99*, 856–858.
[17] Y. Iiduka, T. Wakahara, T. Nakahodo, T. Tsuchiya, A. Sakuraba, Y. Maeda, T. Akasaka, K. Yoza, E. Horn, T. Kato, M. T. H. Liu, N. Mizorogi, K. Kobayashi, ;S. Nagase, *J. Am. Chem. Soc.* **2005**, *127*, 12500–12501.
[18] E. Nishibori, I. Terauchi, M. Sakata, M. Takata, Y. Ito, T. Sugai, H. Shinohara, *J. Phys. Chem. B* **2006**, *110*, 19215–19219.
[19] a) K. Tan, X. Lu, *J. Phys. Chem. A* **2006**, *110*, 1171–1176; b) S. Taubert, M. Straka, T. O. Pennanen, D. Sundholm, J. Vaara, *Phys. Chem. Chem. Phys.* **2008**, *10*, 7158–7168.
[20] T. Kato, *J. Mol. Struct.* **2007**, *838*, 84–88.

 © 2010 Wiley-VCH Verlag GmbH & Co. KGaA, Weinheim

[21] M. Maggini, G. Scorrano, M. Prato, *J. Am. Chem. Soc.* **1993**, *115*, 9798 – 9799.
[22] M. Prato, M. Maggini, *Acc. Chem. Res.* **1998**, *31*, 519 – 526.
[23] T. Cai, Z. X. Ge, E. B. Iezzi, T. E. Glass, K. Harich, H. W. Gibson, H. C. Dorn, *Chem. Commun.* **2005**, 3594 – 3596.
[24] C. M. Cardona, A. Kitaygorodskiy, A. Ortiz, M. A. Herranz, L. Echegoyen, *J. Org. Chem.* **2005**, *70*, 5092 – 5097.
[25] S. R. Wilson, Q. Lu, *J. Org. Chem.* **1995**, *60*, 6496 – 6498.
[26] J. P. Perdew, K. Burke, M. Ernzerhof, *Phys. Rev. Lett.* **1996**, *77*, 3865 – 3868.
[27] B. Delley, *J. Chem. Phys.* **1990**, *92*, 508 – 517.
[28] M. Yamada, T. Wakahara, T. Nakahodo, T. Tsuchiya, Y. Maeda, T. Akasaka, K. Yoza, E. Horn, N. Mizorogi, S. Nagase, *J. Am. Chem. Soc.* **2006**, *128*, 1402 – 1403.
[29] L. Echegoyen, C. J. Chancellor, C. M. Cardona, B. Elliott, J. Rivera, M. M. Olmstead, A. L. Balch, *Chem. Commun.* **2006**, 2653 – 2655.
[30] P. Jakes, K. Dinse, *J. Am. Chem. Soc.* **2001**, *123*, 8854 – 8855.
[31] A. Popov, L. Dunsch, *J. Am. Chem. Soc.* **2008**, *130*, 17726 – 17742.
[32] a) S. F. Yang, P. Rapta, L. Dunsch, *Chem. Commun.* **2007**, 189 – 191; b) P. Rapta, A. A. Popov, S. Yang, L. Dunsch, *J. Phys. Chem. A* **2008**, *112*, 5858 – 5865.

 © 2010 Wiley-VCH Verlag GmbH & Co. KGaA, Weinheim